

Effect of X-Ray Diffractometer Geometrical Factors on the Centroid Shift of a Diffractive Line for Stress Measurement

A. K. Singh and C. Balasingh

Materials Science Division, National Aeronautical Laboratory, Bangalore-17, India

(Received 15 July 1970; in final form 20 January 1971)

Expressions for the centroid shift of a diffraction line due to geometrical factors have been deduced for a diffractometer case in which the specimen surface is inclined to the x-ray beam at an arbitrary angle. Such a geometry is encountered in the determination of residual stress using a diffractometer. The effects of the centroid shift of a diffraction line due to geometrical factors on the stress derived from the diffractometer measurements have been discussed.

I. INTRODUCTION

In order to achieve high resolution and high count rate simultaneously, the modern diffractometers employ Bragg-Brentano focusing using a line source and a pair of Soller slits. The focusing conditions in practice deviate from the ideal in the following respects¹: (a) The specimen surface does not possess the curvature required for focusing. (b) The x rays penetrate into the specimen and diffracted beam of appreciable intensity occurs from the part of the specimen which does not lie on the diffractometer axis. (c) The source and the receiving slit have finite widths. (d) The incident beam has appreciable axial divergence. Further deviations from the ideal conditions may be caused by poor adjustment of the diffractometer with respect to the x-ray source and of the specimen with respect to the diffractometer axis.

Any departure from the ideal conditions of focusing tends to distort the diffraction line profile. A measure of the position of a diffraction line is either the peak maximum or the centroid. In practice, determining the peak position of a line is easier than the centroid. However, mathematically, the effect of geometrical aberrations on the centroid can be more easily calculated since a diffraction maximum is the convolution²⁻⁵ of the profiles due to individual sources of aberrations; and in such a case the centroid is the sum of the centroids of the individual profiles.

The effect of these aberrations on a diffraction maximum has been considered⁴⁻¹³ in detail for the normal diffractometer condition.

However, for the determination of residual¹⁴ macrostresses in polycrystalline solids using an x-ray diffractometer, it is essential to set the specimen making an arbitrary angle to the x-ray beam. In such a case, the diffracted beam is focused (Fig. 1) at a point whose distance from the diffractometer axis is given by

$$R = S \sin(\theta - \psi) / \sin(\theta + \psi), \quad (1)$$

where S is the distance of the source from the diffractometer axis, B is the Bragg angle, and ψ is the angle between the specimen-surface normal and the reflecting-plane normal. In this paper, we have extended Wilson's¹³ method to derive expressions for

the centroid shift of diffraction line due to geometrical factors for a geometry shown in Fig. 1. The errors introduced by the centroid shift in the experimental values of stresses have also been discussed.

II. BASIC EQUATIONS

In this section, the basic approach of Wilson's method¹³ as modified for the present case has been summarized.

A. Choke of Axon

A plane normal to the diffractometer axis and passing through the center of gravity of the source as viewed from the axis defines the equatorial plane. The divergence of the incident x-ray beam in the plane is termed equatorial divergence. The divergence in a plane containing the diffractometer axis and the center of the line source is termed axial divergence. The point of intersection of the axis of the equatorial plane is taken as the origin of coordinates (O in Fig. 2). The vector \vec{S} (joining A to O) in the equatorial plane defines an ideal incident ray. The ideal diffracted ray is defined by a vector \vec{R} . The length of the vector is fixed by Eq. (1). The direction of the vector is defined by the projection on the equatorial plane of the line joining O to B', the center of gravity of the receiving slit. In a properly adjusted instrument, B' will coincide with B.

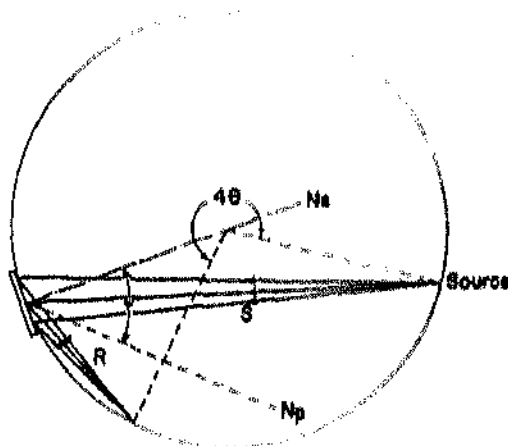


FIG. 1. Focusing geometry when the x-ray beam is inclined to the specimen at an arbitrary angle.

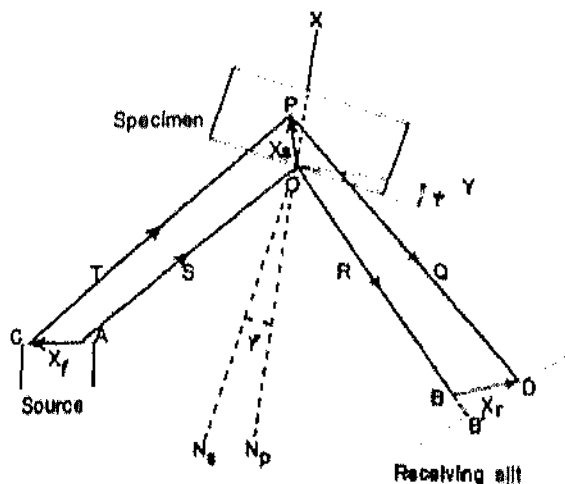


FIG. 2. Definition of the various vectors.

The X and Y axes are chosen in the equatorial plane such that they bisect the angle between \vec{S} and \vec{H} . Z axis is taken perpendicular to X and Y .

A crystallite at O will diffract a ray from A , in the direction on when the diffractometer is set at 2θ , i.e., the angle between \vec{H} and \vec{R} is 2° . Another crystallite situated at a point P in the specimen will diffract a ray T , from C along PD (\vec{Q}) when the diffractometer setting is 2ϕ . 2ϕ differs from 2θ by a small quantity 2ϵ such that $2\phi = 2\theta + 2\epsilon$.

B. Expression for 2ϵ

Let us consider three vectors, \vec{x}_s , \vec{x}_r , and \vec{x}_f , which define a point in the specimen, the source and the receiving slit, respectively. We shall now derive an expression for 2ϵ in terms of these vectors.

From Fig. 2 it is clear that

$$\vec{T} = \vec{S} + \vec{x}_s - \vec{x}_f \quad (2)$$

and

$$\vec{Q} = \vec{R} + \vec{x}_r - \vec{x}_s \quad (3)$$

Since $|\vec{x}_s - \vec{x}_f|/S$ and $|\vec{x}_r - \vec{x}_s|/R$ are small as compared to unity, neglecting the terms in small quantities having powers more than 2, we get

$$T^{-1} = S^{-1} [1 - S^{-2} \vec{S} \cdot (\vec{x}_s - \vec{x}_f) - \frac{1}{2} S^{-2} |\vec{x}_s - \vec{x}_f|^2] \quad (4)$$

and

$$Q^{-1} = R^{-1} [1 - R^{-2} \vec{R} \cdot (\vec{x}_r - \vec{x}_s) - \frac{1}{2} R^{-2} |\vec{x}_r - \vec{x}_s|^2] \quad (5)$$

Since the angle between T and Q is 2ϕ , we have

$$\cos 2\phi = T^{-1} Q^{-1} \vec{T} \cdot \vec{Q} \quad (6)$$

We choose orthogonal components of vectors \vec{x}_s , \vec{x}_r , and \vec{x}_f as follows. The components x_s and y_s of \vec{x}_s are in the equatorial plane and, respectively, perpendicular and parallel to the specimen surface. x_f

and y_f are the components of \vec{x}_f in the equatorial plane and, respectively, parallel and perpendicular to \vec{S} . x_r and y_r are in the equatorial plane and, respectively, parallel and perpendicular to \vec{R} . All the z components are along Z axis.

At this stage, it is necessary to consider the relative magnitudes of the various vector components so that a meaningful approximation may be made. In practice, we have the following conditions governing the relative magnitudes of the components of the vectors \vec{x}_s , \vec{x}_r , and \vec{x}_f :

(a) Since the x-ray beam is strongly absorbed in the specimen, the points with large x_s do not contribute appreciably to the diffracted intensity and thus only the points with $x_s \approx y_s$ and z_s need be considered.

(b) Normally, a line source is used with powder diffractometer. The use of the Soller slit limits the effective value of z_f and is of the order of the separation between the parallel foils of the Soller slit (about 0.5 mm). The focal spot is normally 1×10 mm and when it is viewed at a takeoff angle about $3^\circ - 5^\circ$, $x_f \approx 1$ mm and $y_f \approx 0.05$ mm. Thus, in general, $y_f \approx x_f \approx z_f$.

(c) Similar treatment shows that $y_r \approx z_r$ and y_r is nearly a constant.

On substituting in Eq. (6) the values for \vec{T} , \vec{Q} , T^{-1} , and Q^{-1} from Eqs. (2)–(5) and retaining only the significant terms we get the following expression for 2ϵ :

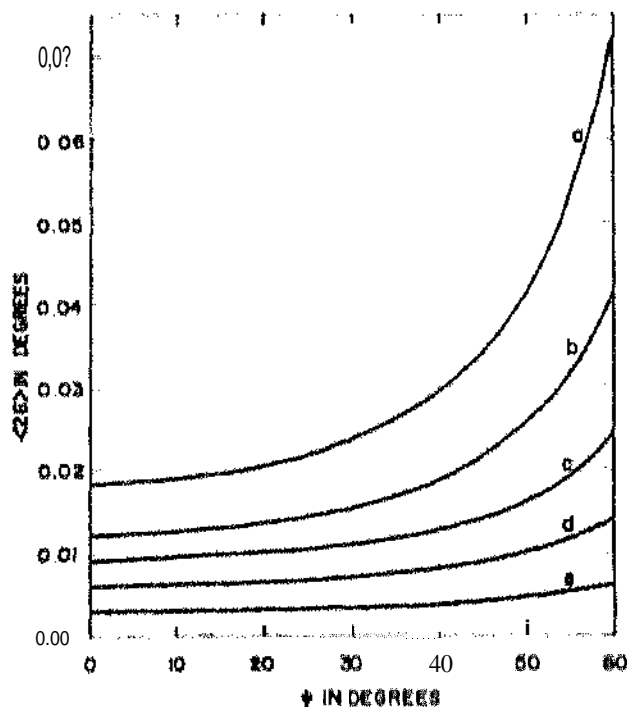


FIG. 3. Plot of $(2\epsilon)_1 + (2\epsilon)_2$ vs ϕ . $\mu = 0.01 \text{ cm}^{-1}$ and $S = 17 \text{ cm}$ have been used to calculate $(2\epsilon)_1$. (a) $\theta = 75^\circ$, $2\alpha = 4^\circ$; (b) $\theta = 80^\circ$, $2\alpha = 4^\circ$; (c) $\theta = 75^\circ$, $2\alpha = 2^\circ$; (d) $\theta = 80^\circ$, $2\alpha = 2^\circ$; (e) $\theta = 85^\circ$, $2\alpha = 2^\circ$. The curve for $\theta = 85^\circ$ and $2\alpha = 4^\circ$ almost overlaps with (d).

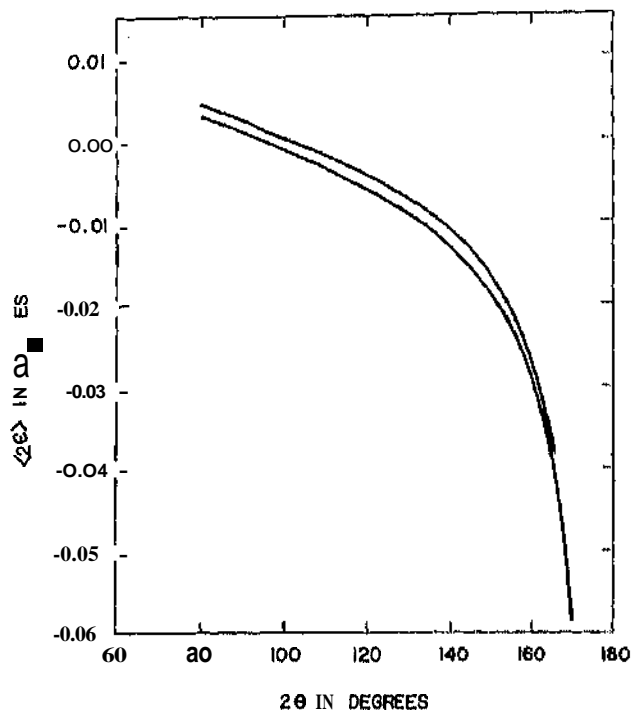


FIG. 4. Plot of $\langle 2\epsilon \rangle_{\text{min}}$ vs 2θ for $q = 1.4$. Upper curve $\psi = 0^\circ$. Lower curve $\psi = 30^\circ$.

$$\begin{aligned}
 2\epsilon = & \eta^{-1} S^{-1} \{ x_s [\cos(\varphi - \psi) + \eta \cos(\varphi + \psi)] + y_r + \eta y_r \} \\
 & + S^{-2} [y_s^2 \eta^{-1} \sin 2\varphi - x_r y_s \sin(\varphi + \psi) - \eta^2 x_r y_s \sin(\varphi - \psi)] \\
 & + \eta^{-1} S^{-2} \{ z_s^2 [1 + \frac{1}{2}(\eta + \eta^{-1}) \cos 2\varphi] \csc 2\varphi + \frac{1}{2} z_r^2 \eta^{-1} \cot 2\varphi \\
 & + \frac{1}{2} z_r^2 \eta \cot 2\varphi - z_r z_s (1 + \eta^{-1} \cos 2\varphi) \csc 2\varphi \\
 & + z_r z_r \csc 2\varphi - z_r z_s (1 - \eta \cos 2\varphi) \csc 2\varphi \}, \quad (7)
 \end{aligned}$$

where

$$\eta = \sin(\theta - \psi) / \sin(\theta + \psi).$$

III. CENTROID SHIFT

A. Equatorial Terms

We shall first consider the terms containing equatorial components.

The terms $y_r/\eta S$ and V^s represent the displacements due to finite width of the source and the receiving slit. The axes of coordinates have been so chosen that

$$\langle y_r \rangle = \langle y_r \rangle = 0.$$

These terms therefore do not lead to any displacement of the centroid.

The term in x_s leads to displacement due to various factors. These include (a) the displacement of the specimen surface from the axis of the diffractom-

eter, (b) tilt of the specimen surface with the diffractometer axis, (c) missetting of I of the 2:1 ratio and the variation of 2:1 ratio, angle, and (d) the finite absorption of the x beam in the specimen.

The displacement of the specimen surface with respect to the diffractometer axis displaces centroid of a diffraction line from its true position. The centre of a diffraction line due to a displacement l of specimen surface from the axis is given by

$$\langle 2\epsilon \rangle_s = l \sin 2\theta / S \sin(\theta - \psi). \quad (8)$$

l is taken to be positive if the diffractometer axis lies outside the specimen and negative otherwise.

The tilt of the specimen with respect to diffractometer axis does not lead to any displacement or small broadening. Similarly, the missetting of 2:1 ratio leads only to broadening.

Due to the finite absorption of x rays in the specimen, diffracted beam of appreciable intensity arises from the material beneath the surface of specimen or, in other words, from the region displaced from the axis of the diffractometer. The displacement of the centroid caused by this is taken by taking the weighted average of the intensity in x_s in 15q. (7) and is given by

$$\langle 2\epsilon \rangle_s = \eta^{-1} S^{-1} [\cos(\varphi - \psi) + \eta \cos(\varphi + \psi)] \langle x_s \rangle, \quad (9)$$

where

$$\langle x_s \rangle = \int_0^t x_s e^{-\mu x_s} dx_s / \int_0^t e^{-\mu x_s} dx_s,$$

where μ is the linear absorption coefficient of specimen for the radiation used, $m = \csc(\varphi - \psi) + \csc(\varphi + \psi)$, and t is the specimen thickness.

On evaluating the integrals, we get

$$\langle x_s \rangle = [1 - \mu m t (e^{-\mu m t} - 1)^{-1}] / \mu m. \quad (10)$$

Even if μ is moderately large, the x-ray beam is absorbed in the specimen within fractions of t and therefore the thickness of the specimen encountered in practice can be taken as infinite. As t tends toward infinity, the second term between square brackets tends toward zero. Thus, for specimen of infinite thickness, we have

$$\langle x_s \rangle = 1 / \mu m. \quad (11)$$

On substituting the value of $\langle x_s \rangle$ from Eq. (11) in (9), we get

$$\langle 2\epsilon \rangle_s = (\eta \mu m S)^{-1} [\cos(\varphi - \psi) + \eta \cos(\varphi + \psi)]. \quad (12)$$

In case μ is small, Eq. (10) instead of (11) must be used for the value of $\langle x_s \rangle$. Additional complications arise if the absorption coefficient is variable. We shall not consider this case as it is not commonly encountered in practice.

The shift of centroid due to term in y_s^2 is given

$$\langle 2\epsilon \rangle_s = \eta^{-1} S^{-2} \sin 2\varphi \langle y_s^2 \rangle. \quad (13)$$

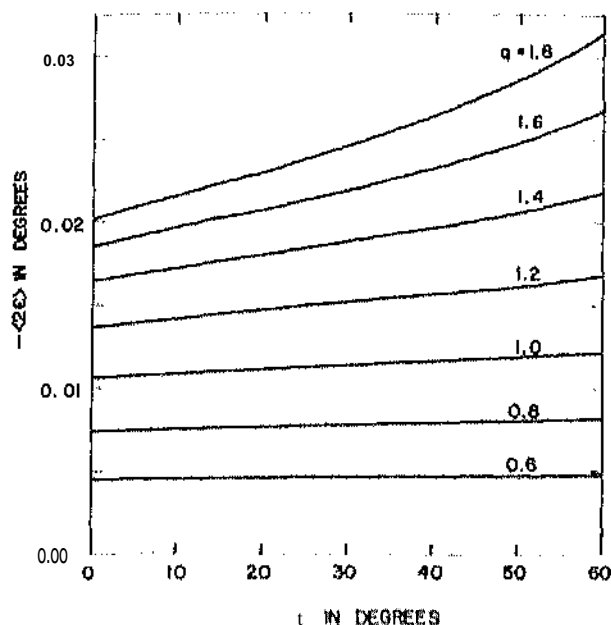


FIG. 5. Plot of $\langle 2\epsilon \rangle_{\text{axial}}$ vs ψ for $\theta = 75^\circ$, $2P = 1$ cm and $S = 17$ cm.

If we assume a uniform distribution of intensity in the primary beam, then

$$\langle y_n^2 \rangle = \frac{\int_{-A_1}^{A_1} y_n^2 dy_n}{\int_{-A_1}^{A_1} dy_n} \quad (14)$$

$$\langle y_n^2 \rangle = \frac{1}{3} (A_1^2 - A_1 A_2 + A_2^2).$$

Since the equatorial divergence 2α is small, we have

$$A_1 \approx A_2 \approx S\alpha / \sin(\varphi + \psi).$$

On substituting the values of A_1 and A_2 , we get

$$\langle 2\epsilon \rangle_3 = \frac{1}{3} \frac{\alpha^2 \sin 2\varphi}{\sin(\varphi + \psi) \sin(\varphi - \psi)}. \quad (15)$$

The term in $x_f y_n$ does not contribute to the displacement of centroid since the axis has been chosen such that $\langle x_f \rangle = 0$ and there is no correlation between x_f and y_n .

The term in $x_f y_n$ will contribute to the displacement of centroid and the broadening. These contributions arise due to the fact that the center of gravity of the illuminated area does not lie on the diffractometer axis and there is small error in the adjustment of the position of the receiving slit on the detector arm. By careful adjustment, these errors can be reduced to about 0.1 mm. With these values, the displacement of the centroid should be less than

$$\langle 2\epsilon \rangle_4 \approx 0.01(\eta S)^{-2} \sin(\varphi - \psi). \quad (16)$$

B. Axial Terms

We shall now derive an expression for the centroid shift arising from the axial terms. The axial terms in Eq. (2) can be rewritten

$$(2\epsilon)_{\text{axial}} = \frac{1}{2} \delta^2 \cot 2\varphi + \frac{1}{2} \nu^2 \cot 2\varphi - \delta \nu \csc 2\varphi, \quad (17)$$

where

$$\delta = (z_s - z_f)/S \quad (18)$$

and

$$\nu = (z_f - z_s)/\eta S. \quad (19)$$

δ and ν represent the angles which incident and the diffracted rays make with the equatorial plane. We shall consider the case of two Soller slits, one in the incident beam and the other in the diffracted beam. The Soller slits limit the maximum axial divergence to A and reduce the intensity by a factor $(1 - |\delta|/\Delta)$ of the rays which make an angle δ with the equatorial plane; A is equal to the separation between the foils of the Soller slits divided by the length of the foil.

The displacement of the centroid is given by

$$\langle 2\epsilon \rangle_{\text{axial}} = N/D, \quad (20)$$

where

$$N = \int \int \int (2\epsilon)_{\text{axial}} (1 - |\delta|/\Delta) (1 - |\nu|/\Delta) d\nu d\delta d\varphi \quad (21)$$

and

$$D = \int \int \int (1 - |\delta|/\Delta) (1 - |\nu|/\Delta) d\nu d\delta d\varphi. \quad (22)$$

It is sufficient¹⁰ to consider only the positive value of δ with both positive and negative values for ν . $f > 1$ is identical with z_s . Following Pike,¹⁰ we introduce a parameter q which is defined as

$$\Delta S = qP,$$

where $2P$ is the axial dimension of the specimen. We shall confine our attention only to the case in which the axial dimensions of the focus, specimen, and the receiving slit are all equal. In practice, one can turn the specimen such that the surface normal

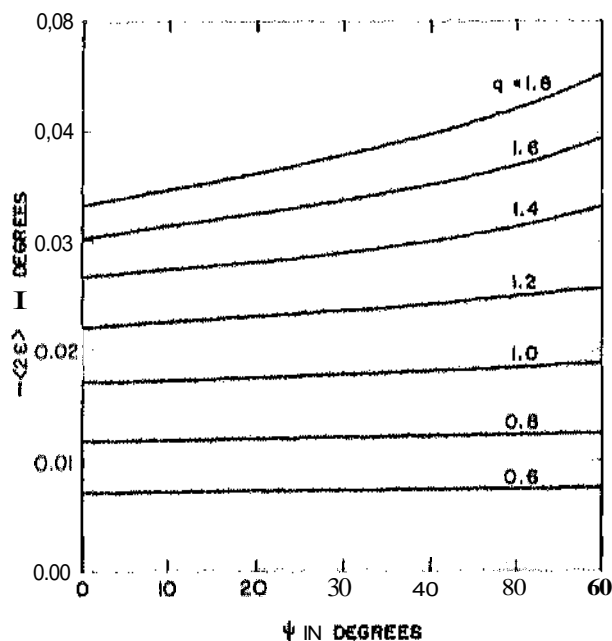


FIG. 6. Plot of $\langle 2\epsilon \rangle_{\text{axial}}$ vs ψ for $\theta = 80^\circ$, $2P = 1$ cm and $S = 17$ cm.

TABLE I. Estimation of $\Delta\sigma^a$ for a few materials, $S=17$ cm, $q=1.4$, and $2P=1$ cm have been used in the calculations. These values are for a Norelco powder diffractometer.

Material	Radiation (hkl)	$2\theta^\circ$	$2\alpha^\circ$	$K_{(0-45)}$ ksi/ $^\circ\Delta 2\theta$	$\langle 2\epsilon \rangle_0 - \langle 2\epsilon \rangle_{45}$	$\Delta\sigma$	$K_{(0-60)}$ ksi/ $^\circ\Delta 2\theta$	$\langle 2\epsilon \rangle_0 - \langle 2\epsilon \rangle_{60}$	$\Delta\sigma$
Steel AISI 4340	CrK α (211)	156	4	120	-0.0073	-0.8760	HO	-0.0305	-2.4400
			1		+0.0029	+0.3480		+0.0032	+0.2560
Titanium alloy Ti-6Al-4V	CuK α (2133)	150	}	70	-0.0111	-0.7770	47	-0.0462	-2.1714
					+0.0024	+0.1680		+0.0017	+0.0799
Aluminum alloy 7079-T611	CrK α (311)	140	4	"	-0.0198	-0.9900	33	-0.0924	-3.0492
			1		+0.0010	+0.0500		-0.0029	-0.0957
Aluminum alloy 7079-T611	CuK α (333)	162	I	-	-0.0045	-0.0900	13	-0.0194	-0.2522
					+0.0028	+0.0500		+0.0036	+0.0468

^aIn calculating $\langle 2\epsilon \rangle_0$ and $\langle 2\epsilon \rangle_{45}$, same value of 20 has been used. The numerical values therefore, correspond to a limiting case when the specimen is stress free. In the presence of any stress, 200 and $2\theta_0$ will differ slightly.

moves either towards the source (as shown in Fig.

1) or away from it; the position of the receiving slit moves respectively closer to or farther from the diffractometer axis. For various practical reasons, the former setting is chosen. This gives $\eta \leq 1$. We shall, therefore, consider only $\eta \leq 1$ in the further discussions. The expressions for $\langle 2\epsilon \rangle_{\text{axial}}$ for the various cases are given in the Appendix.

IV. DISCUSSION

The total displacement of the centroid of a diffraction line is given by the sum of the displacements

due to the various terms in Eq. (7). Among the contributions arising from the equatorial terms, $\langle 2\epsilon \rangle_1$ and $\langle 2\epsilon \rangle_4$ can be made negligible by the proper adjustment of the specimen and diffractometer. The main sources of displacement of the centroid are then, the specimen transparency and the divergence of the beam. A plot of $\langle 2\epsilon \rangle_2 + \langle 2\epsilon \rangle_3$ against μ is shown in Fig. 3 for a few q and 2α values. $\mu = 140$ cm⁻¹ and $S = 17$ cm have been used in the computation of $\langle 2\epsilon \rangle_2$. Both $\langle 2\epsilon \rangle_2$ and $\langle 2\epsilon \rangle_3$ are positive and therefore the total displacement is toward low θ value. Since μ occurs in the denominator [Eq. (12)], $\langle 2\epsilon \rangle_2$ be-

TABLE II. Limits of δ , v , and p used in Eqs. (21) and (22).

(I) $q \geq 2$ and $\eta q \geq 2$		
$0 \leq \delta \leq (P+p)/S$	$-P \leq p \leq +P$	$-(P+p)/\eta S \leq v \leq (P-p)/\eta S$
(II) $q \geq 2$ and $1 \leq \eta q \leq 2$		
$0 \leq \delta \leq (P+p)/S$	$-P \leq p \leq P(1-\eta q)$	$-(P+p)/\eta S \leq v \leq A$
$0 \leq \delta \leq (P+p)/S$	$P(1-\eta q) \leq p \leq -P(1-\eta q)$	$-(P+p)/\eta S \leq v \leq (P-p)/\eta S$
$0 \leq \delta \leq (P+p)/S$	$-P(1-\eta q) \leq p \leq +P$	$-\Delta \leq v \leq (P-p)/\eta S$
(III) $q \geq 2$ and $\eta q \leq 1$		
$0 \leq \delta \leq (P+p)/S$	$-P \leq p \leq -P(1-\eta q)$	$-(P+p)/\eta S \leq v \leq A$
$0 \leq \delta \leq (P+p)/S$	$-P(1-\eta q) \leq p \leq P(1-\eta q)$	$-A \leq v \leq A$
$0 \leq \delta \leq (P+p)/S$	$P(1-\eta q) \leq p \leq +P$	$-\Delta \leq v \leq (P-p)/\eta S$
(IV) $1 \leq q \leq 2$ and $1 \leq \eta q \leq 2$		
$0 \leq \delta \leq (P+p)/S$	$-P \leq p \leq P(1-\eta q)$	$-(P+p)/\eta S \leq v \leq A$
$0 \leq \delta \leq (P+p)/S$	$P(1-\eta q) \leq p \leq -P(1-\eta q)$	$-(P+p)/\eta S \leq v \leq (P-p)/\eta S$
$0 \leq \delta \leq (P+p)/S$	$-P(1-\eta q) \leq p \leq -P(1-q)$	$-\Delta \leq v \leq (P-p)/\eta S$
$0 \leq \delta \leq \Delta$	$-P(1-q) \leq p \leq +P$	$-\Delta \leq v \leq (P-p)/\eta S$
(V) $1 \leq q \leq 2$, $\eta q \leq 1$ and $(q+\eta q) \geq 2$		
$0 \leq \delta \leq (P+p)/S$	$-P \leq p \leq -P(1-\eta q)$	$-(P+p)/\eta S \leq v \leq A$
$0 \leq \delta \leq (P+p)/S$	$-P(1-\eta q) \leq p \leq P(1-\eta q)$	$-\Delta \leq v \leq A$
$0 \leq \delta \leq (P+p)/S$	$P(1-\eta q) \leq p \leq -P(1-q)$	$-\Delta \leq v \leq (P-p)/\eta S$
$0 \leq \delta \leq \Delta$	$-P(1-q) \leq p \leq P$	$-\Delta \leq v \leq (P-p)/\eta S$
(VI) $1 \leq q \leq 2$ and $\eta q \leq 1$ and $(q+\eta q) \leq 2$		
$0 \leq \delta \leq (P+p)/S$	$-P \leq p \leq -P(1-\eta q)$	$-(P+p)/\eta S \leq v \leq A$
$0 \leq \delta \leq (P+p)/S$	$-P(1-\eta q) \leq p \leq -P(1-q)$	$-\Delta \leq v \leq A$
$0 \leq \delta \leq \Delta$	$-P(1-q) \leq p \leq P(1-\eta q)$	$-\Delta \leq v \leq A$
$0 \leq \delta \leq \Delta$	$P(1-\eta q) \leq p \leq P$	$-\Delta \leq v \leq (P-p)/\eta S$
(VII) $q \leq 1$ and $\eta q \leq 1$		
Same as (VI)		

comes appreciable only when μ is low. For a given value of θ and 2α , the displacement of the centroid is minimum at $\psi = 0$ and increases with the increasing value of ψ .

The expressions (given in the Appendix) for the centroid shift due to axial divergence are more complicated. The nature of $(2\epsilon)_{\text{axial}}$ is best understood with the help of Figs. 4 and 5. Figure 4 shows the variation of $(2\epsilon)_{\text{axial}}$ with 2θ for $q = 1.4$ and $\psi = 0^\circ$ and $\psi = 30^\circ$. It is seen that for low 2θ values, $(2\epsilon)_{\text{axial}}$ is positive and decreases with the increasing value of 2θ , passes through zero, and becomes negative for high 2θ values. Thus, for high-angle reflections which are mostly used in stress measurement work, the shift is towards high 2θ value. Figures 5a and 5b show the variation of $(2\epsilon)_{\text{axial}}$ with ψ for $\theta = 75^\circ$ and 80° , respectively.

V. EFFECT ON STRESS MEASUREMENT

It is interesting to estimate the errors introduced by the centroid shift of a diffraction line, in the measured values of stresses. First, we shall consider the effect on the stress factor, which is determined by measuring $(2\theta_0 - 2\theta_g)$ as a function of stress σ , applied to a test specimen.¹⁴ Within the elastic limits a plot of $(2\theta_0 - 2\theta_g)$ vs σ is a straight line. The slope $d\sigma/d(2\theta_0 - 2\theta_g)$ of the line gives the stress factor K . The displacement of the diffraction line will introduce an error $\cdot (2\epsilon)_0 + (2\epsilon)_g$ in $(2\theta_0 - 2\theta_g)$. The error, therefore, will shift the line in σ vs $(2\theta_0 - 2\theta_g)$ plot, parallel to $(2\theta_0 - 2\theta_g)$ axis. This will appear as a spurious residual stress of magnitude $K[(2\epsilon)_0 - (2\epsilon)_g]$. The conclusions are based on the approximation which does not introduce appreciable errors, that $(2\epsilon)_0 - (2\epsilon)_g$ is constant at different stress levels. Thus, to a good approximation the

determination of K is not affected by the centroid shift.

The effect of the centroid shift on the determination of stress is such that

$$\sigma_{\text{true}} = K(2\theta_0 - 2\theta_g) + K[(2\epsilon)_0 - (2\epsilon)_g],$$

$$\sigma_{\text{true}} = \sigma_{\text{obs}} + \Delta\sigma.$$

For a few materials, $\Delta\sigma$ has been estimated and results are summarized in Table 1. It is seen that $\Delta\sigma$ is small if the measurement at $\psi = 0^\circ$ and $\psi = 45^\circ$ are made and 2α is 1° .

The corrections become appreciable for $2\alpha = 4^\circ$. The measurements are often made at $\psi = 0^\circ$ and $\psi = 60^\circ$ to achieve better sensitivity. The corrections in this case become appreciable especially for $\mu > 4^\circ$.

CONCLUSION

The expressions derived in this paper enable us to calculate the shift of the centroid of a diffraction maximum for a diffractometer geometry used in the determination of residual stresses. This analysis may serve as a useful guideline in selecting various parameters such as the equatorial and the axial divergences to minimize the errors. In cases this cannot be done because either it results in a considerable drop of intensity or the proper sizes of all systems are not readily available, the errors can be calculated and a correction applied if found appreciable.

ACKNOWLEDGMENTS

The authors wish to thank Dr. S. Ramaseshan and Dr. S.R. Valluri for their encouragement and keen interest in the work.

APPENDIX

The limits of the integrals in Eqs. (21) and (22) under various conditions are given in Table II. On evaluating the integrals we find that the expressions for $(2\epsilon)_{\text{axial}}$ are identical for cases II and III and for IV and V. The expressions (with a notation $q = a$) for the various cases are given below:

Case I, $q > 2$ and $\eta > 2/q$:

$$(2\epsilon)_{\text{axial}} = (r^2/S^2) \left[\eta^{-2} \left(-\frac{1}{2}a + \frac{1}{2}a^2 \right) + \eta^{-2} \left(\frac{1}{2}a - \frac{1}{2}a^2 \right) + \eta^{-1} \left(-\frac{1}{2}a + \frac{1}{2}a^2 \right) + \left(\frac{1}{105} - \frac{1}{5}a \right) \cot 2\psi - \left[\eta^{-2} \left(\frac{1}{2}a - \frac{1}{2}a^2 \right) + \eta^{-1} \left(-\frac{1}{2}a + \frac{1}{2}a^2 \right) \right] \csc 2\psi \right] \left[\eta^{-2} \left(-\frac{1}{2}a + \frac{1}{2}a^2 \right) + \frac{1}{15} - \frac{1}{5}a \right]^{-1}. \quad (23)$$

Case II, $q > 2$ and $\eta < (2/q - 1)$:

$$(2\epsilon)_{\text{axial}} = (r^2/S^2) \left[\eta^{-2} \left(\frac{1}{2}a^2 - \frac{1}{2}a^4 \right) + \eta^{-2} \left(-\frac{1}{2}a^2 + \frac{1}{2}a^4 \right) - \frac{1}{2}a^2 + \frac{1}{2}a^4 + \eta^{-1} \left(\frac{1}{2}a - \frac{1}{2}a^2 + \frac{1}{2}a^3 - \frac{1}{2}a^5 \right) + \left(-\frac{1}{2} + \frac{1}{2}a \right) \cot 2\psi - \left[\eta^{-2} \left(\frac{1}{2}a^2 - \frac{1}{2}a^4 \right) + \eta^{-1} \left(\frac{1}{2}a - \frac{1}{2}a^2 + \frac{1}{2}a^3 - \frac{1}{2}a^5 \right) \right] \csc 2\psi \right] / \left[\eta^{-2} \left(2a - \frac{1}{2}a^2 \right) + \left(-\frac{1}{2} + \frac{1}{2}a - \frac{1}{2}a^2 + \frac{1}{2}a^4 \right) \right]. \quad (24)$$

Case III, $1 < q < 2$ and $\eta > (2/q - 1)$:

$$(2\epsilon)_{\text{axial}} = (r^2/S^2) \left[\eta^{-2} \left(\frac{1}{2}a^2 - \frac{1}{2}a^4 \right) + \eta^{-2} \left(-\frac{1}{2}a^2 + \frac{1}{2}a^4 \right) + \eta^{-1} \left(\frac{1}{2}a^2 - \frac{1}{2}a^4 + \frac{1}{2}a^6 \right) + \eta^{-1} \left(-\frac{1}{2}a^2 + \frac{1}{2}a^4 - \frac{1}{2}a^6 \right) + \frac{1}{2}a^2 - \frac{1}{2}a^4 + \frac{1}{2}a^6 + \eta^{-2} a^{-1} \left(\frac{1}{2}a - \frac{1}{2}a^2 + \frac{1}{2}a^3 - \frac{1}{2}a^5 \right) + \eta^{-2} a^{-1} \left(-\frac{1}{2}a + \frac{1}{2}a^2 - \frac{1}{2}a^3 + \frac{1}{2}a^5 \right) + \eta^{-1} a^{-1} \left(\frac{1}{2}a - \frac{1}{2}a^2 + \frac{1}{2}a^3 - \frac{1}{2}a^5 \right) + \eta^{-1} a^{-1} \left(-\frac{1}{2}a + \frac{1}{2}a^2 - \frac{1}{2}a^3 + \frac{1}{2}a^5 \right) \right] \cot 2\psi - \left[\eta^{-2} \left(\frac{1}{2}a^2 - \frac{1}{2}a^4 \right) + \eta^{-1} \left(\frac{1}{2}a^2 - \frac{1}{2}a^4 + \frac{1}{2}a^6 \right) \right] \csc 2\psi$$

$$\begin{aligned}
& + \eta^{-6}(-\frac{1}{10}a^3 + \frac{1}{20}a^4) + \eta^{-6}(\frac{2}{3}a^2 - \frac{1}{6}a^3 + \frac{1}{12}a^5) + \eta^{-4}(-\frac{2}{3}a + \frac{2}{3}a^2 - \frac{1}{10}a^4) + \eta^{-2}a^{-1}(\frac{9}{15} - \frac{1}{15}a + \frac{2}{3}a^3 - \frac{1}{6}a^4 + \frac{1}{30}a^5) \\
& + \eta^{-1}a^{-2}(-\frac{32}{15} + \frac{8}{15}a - \frac{2}{3}a^3 + \frac{2}{3}a^4 - \frac{1}{10}a^6 + \frac{1}{15}a^6 - \frac{1}{252}a^7) \} \csc 2\varphi \} / [\eta^{-5}\frac{1}{20}a^3 + \eta^{-4}(-\frac{1}{12}a^2 + \frac{1}{24}a^3) \\
& + \eta^{-3}(\frac{1}{3}a - \frac{1}{3}a^2 - \frac{1}{12}a^3) + \eta^{-2}(-\frac{2}{3} + a + \frac{1}{2}a^2) + \eta^{-1}a^{-1}(\frac{2}{3} - \frac{4}{3}a + a^2 - \frac{1}{3}a^3) - \eta^{-8}(-\frac{1}{15} + \frac{2}{3}a - \frac{2}{3}a^2 + \frac{1}{3}a^3 - \frac{1}{15}a^4 \\
& + \frac{1}{60}a^5)].
\end{aligned}
\tag{25}$$

use IV. $q \leq 2$ and $\eta \leq (2/q - 1)$:

$$\begin{aligned}
\langle 2\epsilon \rangle_{\text{axial}} = (P^2/S^2)a^2 [(\frac{1}{1600} - \frac{1}{720}\eta^{-1} + \frac{1}{504}\eta^{-2} - \frac{1}{120}\eta^{-3} + \frac{1}{3}\eta^{-4}a^{-1} - \frac{7}{360}\eta^{-4} - \frac{7}{180}\eta^{-5}) \cot 2\varphi - (\frac{1}{504}\eta^{-1} + \frac{1}{160}\eta^{-2} \\
- \frac{1}{72}\eta^{-4}) \csc 2\varphi] / [\frac{1}{120} - \frac{1}{24}\eta^{-1} + \eta^{-2}a^{-1} - \frac{1}{12}\eta^{-2} - \frac{1}{3}\eta^{-3}].
\end{aligned}
\tag{26}$$

The aberrations caused by spectral dispersion, refraction, and variation of response with wavelength have not been considered.

R. C. Spencer, *Phys. Rev.* 55, 239 (1939).
 R. C. Spencer, *J. Appl. Phys.* 20, 413 (1949).
 L. Alexander, *J. Appl. Phys.* 21, 126 (1950).
 L. Alexander, *J. Appl. Phys.* 25, 155 (1954).
 L. Alexander, *J. Appl. Phys.* 19, 1068 (1948).
 L. Alexander, *Brit. J. Appl. Phys.* 4, 92 (1953).
 A. J. C. Wilson, *J. Sci. Instr.* 27, 327 (1950). In stress measurement work peak of a diffraction line is taken as a measure of position. The displacement of the peak to a first approximation is same [A. J. C. Wilson, *Proc. Phys. Soc. (London)* 78, 249 (1961)] as that of the centroid. The physical aberrations which are not discussed

in this paper may effect the peak and the centroid quite differently (Ref. 13).

⁹J. N. Estabrook, *Brit. J. Appl. Phys.* 3, 349 (1952).

¹⁰E. R. Pike, *J. Sol. Instr.* 24, 355 (1957).

¹¹J. I. Langford, *J. Sci. Instr.* nil, 515 (1962).

¹²B. Gale, *Brit. J. Appl. Phys.* 29, 64 (1958).

¹³A. J. C. Wilson, *Mathematical Theory of Powder Diffraction* (Phillips Technical Library, Netherlands, 1963).

¹⁴B. D. Cullity, *Elements of X-Ray Diffraction* (Addison-Wesley, New York, 1959), p. 431.

¹⁵D. N. French, *J. Am. Ceram. Soc.* 52, 271 (1969) (see Appendix).

¹⁶M. E. Millberg, *J. Appl. Phys.* 41, 64 (1968).